Microscopic structural changes of SiO_2 glasses as a function of temperature investigated by *in situ* Raman spectroscopy

N. Shimodaira
Research Center, Asahi Glass Co. Ltd., 1150 Hazawa-cho, Kanagawa-ku, Yokohama 221-8755, Japan

K. Saito, E. H. Sekiya, and A. J. Ikushima
Research Center for Advanced Photon Technology, Toyota Technological Institute, 2-12-1 Hisakata, Tempaku, Nagoya 468-8511, Japan
(Received 21 March 2006; revised manuscript received 16 May 2006; published 19 June 2006)

In situ Raman spectroscopic measurements with a useful peak deconvolution technique were attempted in this paper to quantitatively investigate the structural changes of silica glass as a function of temperature in the range from room temperature to 1300 °C. By utilizing an F-doped silica glass having a fictive temperature $T_f(=T_g)=700$ °C, we have made clear observations of the structural relaxation in the supercooled liquid state as well as the thermal expansion in the glassy state. From the frequency shift of fundamental vibrations with the increase of temperature, it was deduced that the decreases of both the Si-O-Si average bond angle θ and the Si-O bond-stretching force constant α simultaneously occur by thermal expansion. Contrary to a previous report, the rates of change of band frequencies with temperature are definitely less sensitive to T_g, while the D_2 (and D_1) intensity explicitly increases above T_g. The activation energy of D_2 formation was determined by using actual temperature to be 0.43 ± 0.02 eV, which is close to the previously obtained ones in pure silica glass by using T_f evaluated at room temperature. Based on the central-force network model and the so-called "Badger's law," it was evaluated from the shift of ω_4 frequency that the rate of change of θ as a function of temperature, $\Delta\theta/\Delta T$, is approximately $-0.02°/°C$, and is a few times larger than $\Delta\theta/\Delta T_f$, approximately $-0.005°/°C$. The intrinsic mechanism of the angular change with T_f in silica glass is also explained from these results.

DOI: 10.1103/PhysRevB.73.214206 PACS number(s): 61.43.Fs, 63.50.+x, 78.30.Ly, 65.60.+a

I. INTRODUCTION

Structure, physical properties, and performances of glass materials are determined at the glass transition temperature T_g. Thus *in situ* investigations of high-temperature properties across T_g are very important to clarify the nature of glass. However, in silica glass, measurements are by no means free from difficulty due to the high T_g, typically over 1000 °C,[1] and in addition, calorimetric or volume measurement cannot determine the T_g. Only recently, *in situ* light scattering[2] and *in situ* small-angle x-ray scattering (SAXS) (Ref. 3) have clearly detected the change of intensities at T_g, and the vacuum ultraviolet (VUV) absorption measurement has also been reported over a wide temperature range across T_g,[4] whereas vibrational spectroscopy has not necessarily given valuable information at such high temperatures so far, though it is the most useful tool for understanding the microscopic structure of glass in the short-to-medium-range order.

Accordingly, the structure and properties of silica glass are investigated in most cases, for convenience, as a function of the fictive temperature T_f, which is determined at room temperature as the "frozen-in" temperature where the structure and properties of glass are the same as those of the supercooled liquid. When the sample reaches an equilibrium state at respective heat-treatment temperatures and is quenched, T_f defined as the heat-treatment temperature (T) becomes a good indicator of the glass structure, corresponding to T_g.

According to this basic principle, the changes of structure and properties in silica glasses have been systematically investigated by changing the T_f. For example, the position of an infrared (IR) absorption around 2260 cm^{-1}, corresponding to an overtone band ascribed to the Si-O-Si asymmetric stretching vibrational mode, was found to have a linear relationship with T_f, indicating the average magnitude of Si-O-Si bond angles: the smaller wave number corresponds to the smaller average bond angle.[5] Thus T_f can be easily determined at room temperature, developing an understanding of relationships with the light scattering,[6] SAXS,[2,7] the Urbach edge,[8] the Boson peak in Raman scattering,[9] and so on.

Concerning Raman spectroscopic investigations as well, structural changes in silica glass as a function of T_f were studied in detail. Based on a central-force network dynamics model (CFNM),[10,11] it was suggested by Geissberger *et al.*[12] that (i) the Raman bands, assigned to fundamental skeletal vibrations labeled ω_1 (about 420 cm^{-1}), ω_3 (about 800 cm^{-1}), and ω_4 (about 1060 cm^{-1} for TO and about 1200 cm^{-1} for LO, respectively), shift in frequency in a manner with the change of T_f. The result was interpreted as that the average Si-O-Si angle θ decreases with increasing T_f. (ii) The sharp "defect" lines, D_1 (495 cm^{-1}) and D_2 (605 cm^{-1}), show little shift in frequency. (iii) Both the D_1 and D_2 intensities increase with T_f and exhibit the Arrhenius behavior, $\exp(-\Delta E/k_B T_f)$, with activation energies of the "formation," $\Delta E=0.14$ and 0.40 eV, respectively. Consequently, from the agreement of the experimental and predicted values,[13] they assigned the D_1 and D_2 lines to regular (possibly puckered) fourfold and planar threefold ring structures.

As referred to above, the structure of silica glass evaluated at room temperature has been deeply understood so far. On the contrary, there are only a few *in situ* Raman or IR studies of vitreous or crystalline SiO_2 at temperatures over

1000 °C.[14–17] Among them, McMillan *et al.*[17] reported on the structural changes of pure silica glass as a function of temperature up to 1950 K that (i) the principal low-frequency Raman band (corresponding to ω_1) shows an increase in frequency with increasing temperature, indicating that the average Si-O-Si angle narrows, and further increase above T_g because of configurational changes. (ii) There is an increase in the intensity of the 606-cm^{-1} band (D_2) above T_g. However, the result seems to be unsatisfactory quantitatively, because they did not deal with the complicated Raman spectral shape, and even for temperatures below T_g the spectra seems too noisy to understand the behaviors because of thermal radiation.

Recently, the structure, the structural relaxation, and the VUV absorption edge have been investigated in silica glasses with different fluorine concentrations.[8] According to it, structural relaxation is strongly stimulated by F-doping as previously indicated.[18] In the experiment we have handled samples with lower T_f's than ever expected, reaching T_f =550 °C for the 7.2 mol % F-doped sample. It should be noted that this is an extraordinarily low value compared with that of a typical pure silica glass, usually no lower than T_f =900 °C.[19] At the same time, it can be said that by utilizing an F-doped silica glass sample having such a low T_f, we have got an opportunity to possibly make clear *in situ* observations of the structural changes by vibrational spectroscopy at temperatures across T_g.

In this study we attempt *in situ* Raman spectroscopy and an unprecedented peak deconvolution for the spectra over a wide frequency range. The technique is used for the investigation of microscopic and quantitative changes of the structure of silica glass, focusing either on the Si-O-Si bond angle or on D_1 and D_2. First, the vibrational changes accompanied by thermal expansion below T_g are separately examined. Second, by utilizing an F-doped silica glass sample having low T_f, the structural relaxation over T_g as well as thermal expansion can be explained. The formation energy of the D_1 and D_2 structures is estimated from the Arrhenius behavior, $\exp(-\Delta E/k_B T)$, where T is the actual temperature. Finally, the intrinsic mechanism of the angular change with T_f in silica glass is discussed from the estimate of θ changes with temperature.

II. EXPERIMENT

A. Experimental procedure

Raman spectra were obtained with a NRS-2100 (JASCO) using an Ar ion laser as the light source operating at 500 mW of the 488-nm line. The laser power, 180 mW on average, was monitored at sample for normalizing the Raman scattering intensity. The vertically polarized laser light irradiated the sample with the incident angle of 30°, and the randomly polarized light ($VV+VH$), pseudobackscattered normal to the sample surface, was analyzed over the range from 10 to 1750 cm^{-1} at approximately 1 cm^{-1} intervals with a triple pass grating monochromator with the spectral slits set in the resolution of approximately 2 cm^{-1}. The detector was a 16-bit charge-coupled device (CCD) cooled by liquid nitrogen.

A commercial hot stage (LK1500, Linkam Scientific Instruments Ltd.) was mounted in the specimen room of the Raman spectrometer. The sample was placed inside a platinum crucible with the size of 8 mm in diameter ×2.5 mm in height, and heated from underneath as well as from the sides. The temperature (T) was controlled by a thermosensor (type S, Pt-10% Rh/Pt thermocouple) set at the bottom of the crucible.

Measurements were performed in air through the silica window from room temperature up to 1300 °C at intervals of 50–200 °C. The heating rate was 10 °C/min. After keeping for 30 min at a desired temperature, measurement of a raw spectrum was initially acquired. The signal acquiring time was 30 min in total. Second, to eliminate the thermal radiation as well as the dark current of the CCD detector, a background spectrum was taken at respective temperature for 30 min, and subtracted from each of the raw spectra. The subtracted spectrum was then normalized by the laser power monitored at the sample just before each measurement of the raw spectrum. Hereafter, the spectrum will be called an experimental spectrum, $I_{\exp}(\omega)$.

Finally, the experimental spectrum was normalized by the thermal population and the scattering absolute frequency dependence in the following form:[20,21]

$$R(\omega) = I_{\exp}(\omega)\frac{\omega}{(n+1)(\omega_0-\omega)^4}, \tag{1}$$

where ω is the Raman frequency shift (cm^{-1}), ω_0 is the absolute frequency of the laser light (20 496 cm^{-1}), $n=[\exp(\hbar\omega/k_B T)-1]^{-1}$ is the Bose-Einstein factor, where $\hbar$ is the Plank constant, k_B is the Boltzmann constant, and T is the absolute temperature for measurement.

B. Samples

Two types of silica glass were prepared by a vapor axial deposition method. One is pure silica glass having T_f =1080 °C, namely "ND." The other is a 5-mol % F-doped sample having T_f=700 °C, namely "F5." F was added by exposing soot of SiO_2 to a fluorine-containing atmosphere. F concentration was evaluated by electron probe microanalysis (EPMA). According to IR absorption measurements, OH concentrations were 1.8×10^{-2} mol % for ND and less than the detection limit for F5, respectively. According to inductively coupled-plasma mass spectrometry analysis (ICPMS), concentrations of metal impurities in the samples, such as Na, K, Fe, Ni, Cu, Mg, Cr, Ti, Al, Li, Zn, Ca, Ce, Mn, Ag, and Pb, were less than 2×10^{-6} mol %. The samples were cut in size of $4\times4\times2$ mm and the surfaces were optically polished.

For ND, temperature was elevated up to 1100 °C mainly to investigate the changes of vibrational and microscopic structures at high temperatures without structural relaxation. On the other hand, temperature was increased up to 1300 °C for F5 to investigate the changes accompanied by structural relaxation.

Table I shows the estimated time of the main structural relaxation, τ, in F5, based on the Arrhenius plots in various F-doped silica glasses.[8] By choosing T_f=700 °C as the ini-

TABLE I. Structural relaxation time τ in F5 (5 mol % F-doped sample) estimated from the Arrhenius plot in Ref. 8.

Temperature (°C)	τ (min)
500	$>1.6\times10^6$
600	8400
650	720
700	110
750	17
800	3.3
850	0.75
900	~0.2
>1000	<0.01

tial state, the structural relaxation during the constant temperature, heating, and measuring process can be ignored when $T \leqslant T_f$, while it progresses and reaches the equilibrium state at T during the heating process when $T > T_f$. That is, F5 having T_f=700 °C is the most convenient sample for the present study.

III. RESULTS

A. Raman spectral changes with temperature

Figure 1(a) represents the experimental spectra for ND at temperatures 27–1100 °C. Peaks are labeled in accordance with CFNM. There are reports pointing out that the peak at about 1200 cm^{-1} does not correspond to a longitudinal optical mode.[22] In this report, it is not handled anymore. With increasing temperatures, the baseline in the region of low frequencies around ω_1 is gradually raised at an apparently constant rate because of the thermal population of phonons. In contrast, as the spectra are normalized by using Eq. (1), the following interesting features come into view with increasing temperature.

In the low-frequency range below 400 cm^{-1}, the normalized spectra coincide well with each other [see Fig. 1(b)]. With ω_1, intensity, position, and width seem to be stable. With ω_3, the measured intensity certainly decreases while the position seems to be stable. With ω_4(TO) and ω_4(LO), the measured intensities decrease while the positions shift to lower frequencies. With D_1 and D_2, the measured intensities apparently decrease while the positions are stable. OT(ω_1), probably ascribed to a markedly broad overtone band of ω_1 centered at about 800 cm^{-1}, grows up with a widely rising baseline from D_1 to ω_4. OT(ω_3), probably ascribed to an overtone band of ω_3 around 1600 cm^{-1}, also grows up.

The normalized spectra for F5 at temperatures 27–1300 °C are shown in Fig. 1(c). Two spectra at 1200 and 1300 °C are shifted upwards for clarity. Many features are basically in common with ND: the noticeable differences observed with F5 are—the measured intensity of D_2 certainly increases from the middle of temperature. The measured intensity of Si-F peak at about 945 cm^{-1} monotonously decreases.

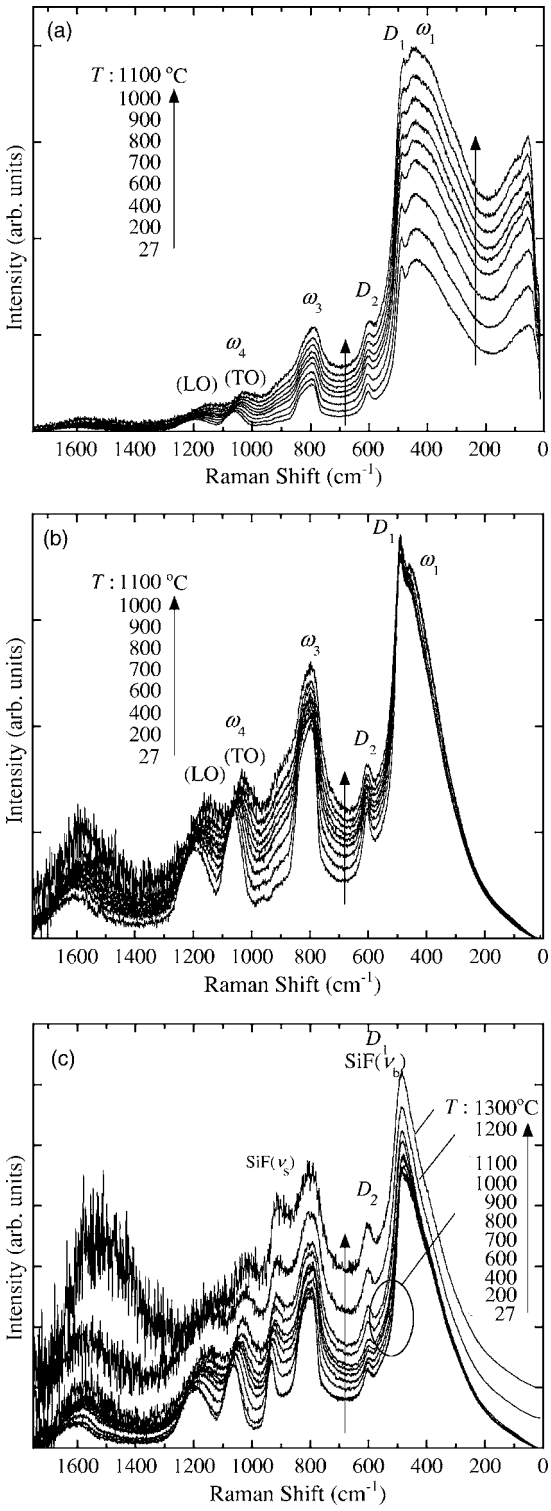

FIG. 1. The experimental Raman spectra of ND at temperatures 27–1100 °C are shown in (a). The normalized spectra of ND and F5 reduced by the thermal population and the scattering absolute frequency dependence in Eq. (1) are shown in (b) and (c), respectively. Two spectra at 1200 and 1300 °C in (c) are shifted upwards for clarity. Allows in the figures subsidiarily show the direction with increasing temperature.

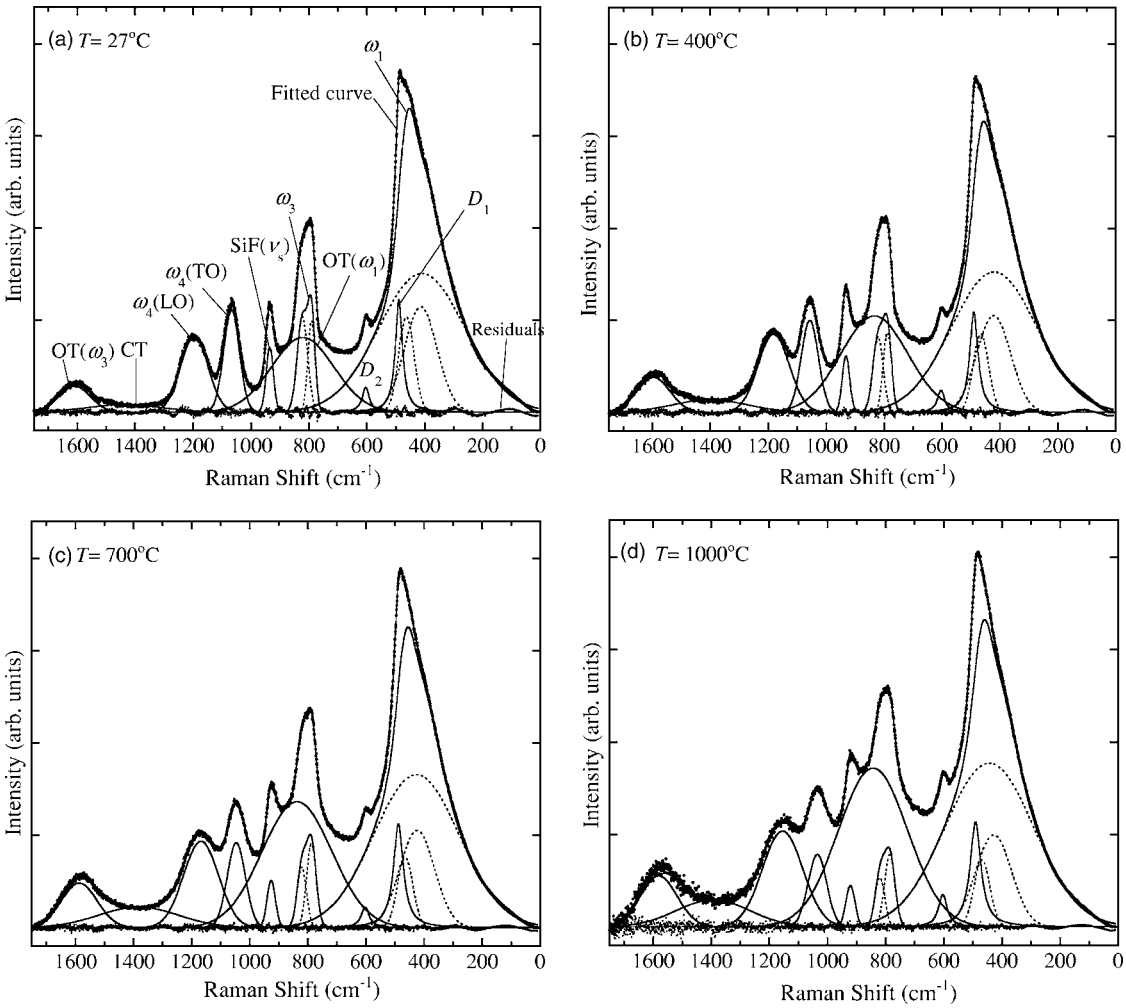

FIG. 2. Results of the peak deconvolution analysis for reduced spectra in F5: (a) 27 °C, (b) 400 °C, (c) 700 °C, and (d) 1000 °C. Three Gaussians for ω_1, two Gaussians for ω_3, one Gaussian for OT(ω_1), SiF(ν_s), ω_4(TO), ω_4(LO), and OT(ω_3), respectively, and one Lorentzian for the D_1 and D_2 lines, respectively, were used. In addition, one more Gaussian for named CT, considered to be due to a combined tone related to ω_1, ω_3, and OT(ω_1), need to be added at about 1400 cm^{-1} to decrease the fitting error. The bending mode of the Si-F bond [SiF(ν_b)] at about 480 cm^{-1} could not be revolved from the D_1 line or a component of the three Gaussian for ω_1 in this fitting procedure. ω_1 and ω_3 peaks were convoluted with three and two Gaussians, respectively.

B. Peak deconvolution

As can be seen in the Raman spectra, overlaps of the peaks as well as the asymmetric shape in some peaks make it difficult to calculate the spectral changes quantitatively. To improve it, based on the peak assignments previously reported, a useful peak deconvolution program over *full* frequencies ranging from 10 to 1750 cm^{-1} has been developed by the author using a commercial package Igor Pro (Wavemetrics), and was conducted in a series of the reduced spectra. The procedure is as follows.

Peaks were generated with model functions, by using Gaussian and Lorentzian: three Gaussians for ω_1, two Gaussians for ω_3, one Gaussian for OT(ω_1), SiF(ν_s), ω_4(TO), ω_4(LO), and OT(ω_3), respectively, and one Lorentzian for the D_1 and D_2 lines, respectively. In addition, one more Gaussian, considered to be due to a combined tone related to ω_1, ω_3, and OT(ω_1), hence named CT, needs to be added at about 1400 cm^{-1} to decrease the fitting error. Strictly speaking, one relatively sharp peak, assigned to the bending mode of the Si-F bond [SiF(ν_b)], also exists at about 480 cm^{-1}. However, it could not be resolved from the D_1 line or a component of the three Gaussians of ω_1 in our fitting procedure.

Then, a total of 39 parameters in maximum, as positions, intensities, and widths of the peaks, are individually adjusted to attain the least value of chi-square by using the popular Levenberg-Marquardst nonlinear least-squares optimization. Examples of the fitting results in F5 are shown in Fig. 2(a) for 27 °C, (b) for 400 °C, (c) for 700 °C, and (d) for 1000 °C, respectively. ω_1 and ω_3 peaks were convoluted with three and two Gaussians, respectively. The correlation (R^2) factor is quite high over 99.9% for temperatures below 1100 °C in both samples, as seen in the residuals in the figure. The standard deviations of the fitted peak parameters were less than 1.5 cm^{-1} in position, 2.5 cm^{-1} in width, and 3% in intensity, respectively.

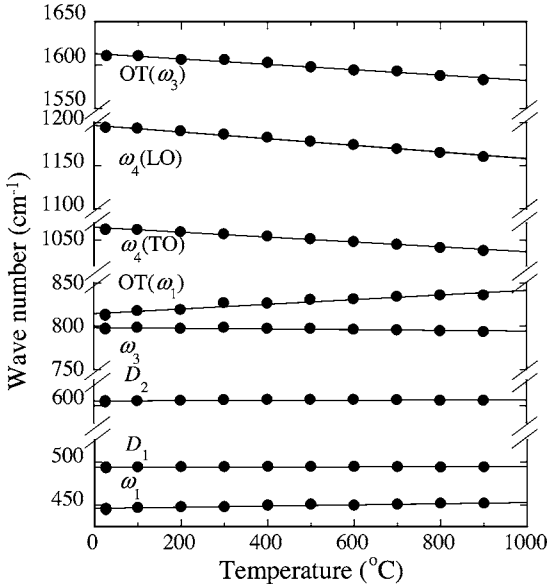

FIG. 3. Plot of the peak frequencies as a function of temperature for ND. The error in all frequencies is estimated to be ±1.5 cm^{-1}. Straight lines in the figure are least-squares fits to the data points, and the parameters of the line, intercept, slope, and correlation (R^2) factor, are given in Table II.

Continuously, the changes of vibrational structure will be sorted out by utilizing these fitted parameters, although a part of them, especially some bands in the high-frequency region for 1200 and 1300 °C in F5, have an uncertainty to some extent because of increasing noise.

C. Frequency variations with temperature

Figure 3 shows the frequencies as functions of temperature for ND. Straight lines in the figure are least-squares fits to the data points, and the parameters of the line, intercept, slope, and R^2 factor, are given in Table II. As far as the R^2 factor, all the peaks except D_1 and D_2 have good linear relationships with temperature. It was clearly found that with increasing temperature, ω_1 shifts to high frequencies while ω_3 and ω_4 shift inversely to low frequencies. Shift directions in overtone bands are in accord with those in their estimated first-order bands.

Interestingly, while the structural relaxation definitely occurs over T_g corresponding to the T_f(=700 °C) for F5, there seems to be no drastic discontinuous points in the same scale of frequencies as Fig. 3. Accordingly, the linear-square fits to the data were attempted in the full range of temperature, and the parameters are also tabulated in Table II. The dependences on temperature are basically very similar to those in ND.

D. Intensity variations with temperature

In both samples, with increasing temperature, overtone bands monotonously and strongly enhance, and ω_1 and ω_4(LO) are relatively stable, and ω_3, ω_4(TO), and SiF(ν_s) in F5 monotonously decrease. As an example, normalized

TABLE II. Parameters of the least-squares linear fitting analysis to the "frequencies vs T" data in (a) for ND (shown in Fig. 3) and (b) for F5, respectively.

(a) ND

Band	Intercept (cm^{-1})	Slope (10^{-3} cm^{-1}/°C)	Correlation coefficient (−)
ω_1	446	7.5	0.954
ω_3	798	−4.1	0.784
ω_4(TO)	1065	−28.7	0.993
ω_4(LO)	1197	−43.4	0.996
D_1	494	0.7	0.346
D_2	606	1.5	0.562
OT(ω_1)	815	27.4	0.967
OT(ω_3)	1613	−31.3	0.987

(b) F5

ω_1	451	8.4	0.893
ω_3	796	−5.1	0.966
ω_4(TO)	1071	−36.2	0.993
ω_4(LO)	1202	−50.0	0.969
D_1	488	2.1	0.572
D_2	603	0.1	0.043
OT(ω_1)	823	21.1	0.987
OT(ω_3)	1612	−33.1	0.970
SiF(ν_s)	938	−16.3	0.989

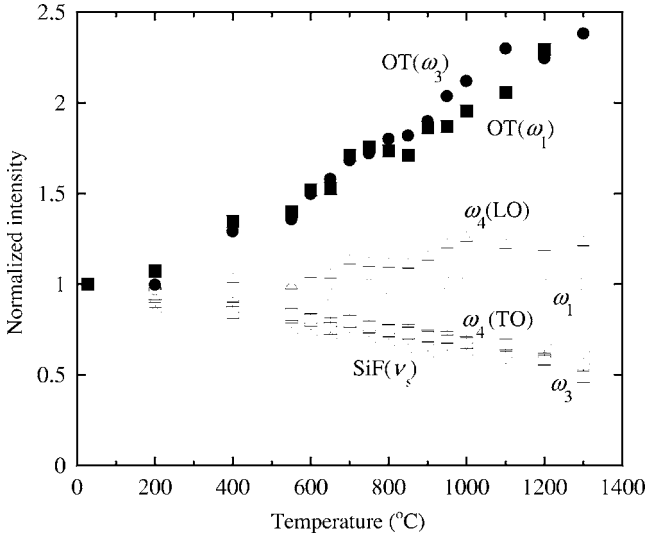

FIG. 4. Plot of the intensity of peaks, ω_1 (open circle), ω_3 (open square), ω_4(TO) (plus), ω_4(LO) (open triangle), OT(ω_1) (filled circle), OT(ω_3) (filled square), and SiF(ν_s) (cross), as a function of temperature in F5. All intensities are normalized at room temperature. The error in all intensities is estimated to be ±3%.

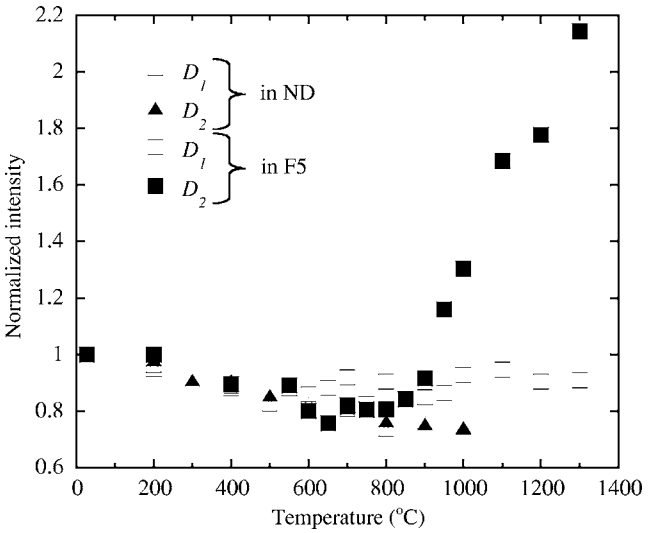

FIG. 5. Plot of the peak intensities of D_1 and D_2 as a function of temperature in ND (square) and F5 (triangle). All intensities are normalized at room temperature. The error in all intensities is estimated to be ±3%.

intensities in F5 except for D_1 and D_2 are plotted as a function of temperature in Fig. 4.

Normalized intensities of D_1 and D_2 in both samples are plotted as a function of temperature in Fig. 5. In ND both the D_1 and D_2 intensities monotonously decrease. On the other hand, it is noticeable in F5 that the D_2 intensity slightly decreases to approximately 700 °C and explicitly turns to increase over the temperature. The D_1 intensity in F5 does not show similar behavior to D_2.

IV. DISCUSSION

In this experiment we attempted *in situ* Raman spectroscopy at high temperatures to directly observe the structural changes including structural relaxation in silica glass. After normalizing the spectra at each temperature by the thermal population, a number of temperature dependences, shift in frequency, change in intensity, etc., could be observed in many bands.

A shift in frequency is one of the typical phenomena accompanied by thermal expansion due to the effect of anharmonic terms. In contrast, positions of D_1 and D_2 are less dependent on temperature. These behaviors strongly lead one to the thought that D_1 and D_2 would be vibrationally isolated in a silica glass structure as indirectly ascribed to small ring structures.

Among the changes in intensity, enhancement of overtone bands is due to the increase of the probability of the multiphonon process at high temperature. Decrease or constancy in intensity of some bands is thought to be due to the relaxation of "crystal" momentum and/or the loss of long-range order at high temperature.

In the present section, based on such changes in vibrational structure observed in Raman spectra, we discuss the structural changes of silica glass at high temperatures accompanied by structural relaxation as well as thermal expansion, focusing on the Si-O-Si bond angle and the D_1 and D_2 structures. Finally, let us consider the intrinsic mechanism of the angular changes with temperature and fictive temperature, based on the quantitative estimation.

A. Si-O-Si average bond angle θ

As shown in Table II, with increasing T, ω_1 shifts to higher frequencies while ω_3 and ω_4 inversely to lower frequencies. According to a central-force network dynamics model (CFNM), which is commonly accepted in silica glass, the Raman frequencies of ω_1, ω_3, and ω_4 are predicted to be dependent on the Si-O-Si bridging bond angle θ by the following equations

$$\omega_1^2 = (\alpha/m_O)(1+\cos\theta), \tag{2}$$

$$\omega_3^2 = (\alpha/m_O)(1+\cos\theta) + 4\alpha/3m_{Si}, \tag{3}$$

$$\omega_4^2 = (\alpha/m_O)(1-\cos\theta) + 4\alpha/3m_{Si}, \tag{4}$$

where α is the Si-O bond-stretching force constant, and m_O and m_{Si} are the masses of the oxygen and silicon atoms, 16 and 28 (g/mol), respectively.

It may be possible to first consider the occurrence of only the increase of the Si-O bond length accompanied by thermal expansion, resulting in the decrease of α. In this case, all the ω's are expected to shift to lower frequencies unanimously. However, the slope of ω_1 is obviously positive in our experiment, implying that the decrease of θ is absolutely required in Eq. (2). Inversely, if only the decrease of θ occurs, ω_1 and ω_3 are expected to shift to higher frequencies, while the slope of ω_3 is negative in our experiment, indicating that the decrease of α is also required in Eq. (3). Consequently, in order to satisfy all the Eqs. (2)–(4), it is necessary that the decreases of both θ and α simultaneously occur by thermal expansion.

Next, let us examine the effect of structural relaxation on the change of θ in more detail by focusing on ω_4, because the band, well isolated in position and symmetric in shape, is the most useful for analysis. Figures 6(a) and 6(b) show the T dependences of position and width of ω_4 (TO) in F5, respectively. For a comparison, the T_f dependences evaluated at room temperature in the 4.0-mol % F-doped sample,[9] namely "F4," are also plotted on the same scale. The dotted lines are guides for the eye.

In Fig. 6(a), the rate of change of the position with T is a few times higher than that with T_f. Note that the rate is less sensitive to T_g, i.e., the occurrence of structural relaxation. This implies that the Si-O-Si average bond angle narrows at an approximately constant rate, irrespective of the progress of configurational changes above T_g such as the formation of D_1 and D_2. It disagrees with the previous report by McMillan *et al.*[17]

They reported that (i) configurational changes at temperatures above T_g result in *further* increase of ω_1 frequency by approximately a factor of 2. (ii) $\Delta\theta$ is −2° at 1500 K and −6° at 2000 K on the assumption that θ decreases by 1° per 10-cm^{-1} shift from ω_1 with reference to CFNM. However, it is obvious that the measured peak position of ω_1 in the nor-

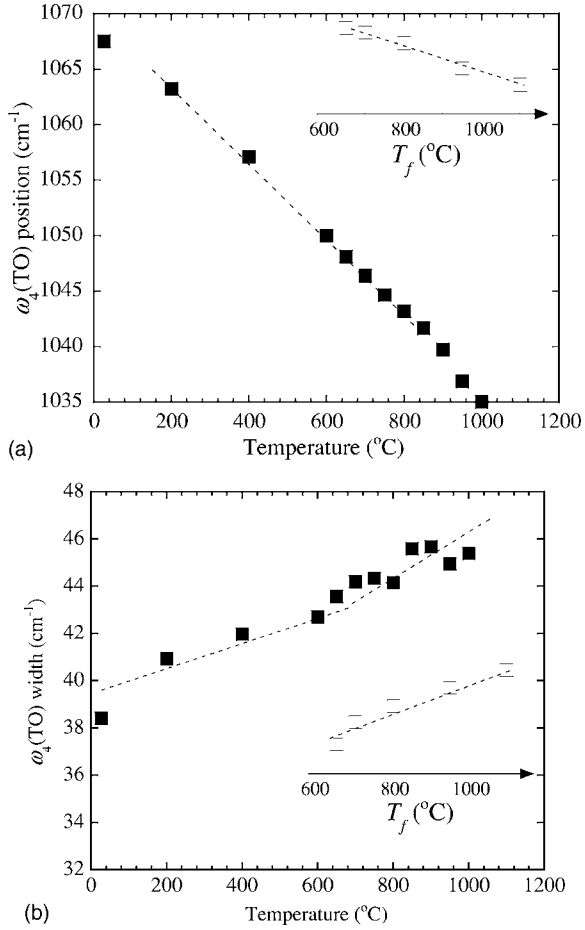

FIG. 6. T dependences of (a) position and (b) width of ω_4(TO) band in F5. T_f dependences in F4 (4 mol % F-doped sample) are also plotted on the same scale. The dotted lines are guides for the eye. The errors are estimated ±1.5 cm^{-1} in position and ±2.5 cm^{-1} in width, respectively.

malized spectra in their report is much less accuracy because of the overlap of ω_1 and D_1 bands, as can be also seen in Figs. 1(b) and 1(c). Therefore their description of the estimation of $\Delta\theta$ from ω_1 frequency also lacks accuracy. In addition, the ω_4 bands in their report could no longer be distinguished even below T_g because of thermal radiation, though ω_4 is the most useful for analysis. On the contrary, it has been clearly proved in Table II and Fig. 6(a) that the rates of change of band frequencies with T are definitely less sensitive to the occurrence of structural relaxation. The quantitative estimate of θ change with T will be discussed later in comparison with T_f.

In Fig. 6(b), the slope of the width in T dependence is approximately the same as that in T_f dependence while it slightly deviates from the dotted line and increases above T_g. The former implies that contributions of thermal vibrations and frozen-in structural disorder to the scattering of the Si-O-Si bond angles are comparable. The latter means that contribution of the dynamic structural disorder over T_g to the scattering of the Si-O-Si bond angle is quite smaller than that of thermal vibrations. These results are similar to the temperature dependences of the absorption edge,[4] in which the contributions of thermal vibrations to the Urbach tail energy

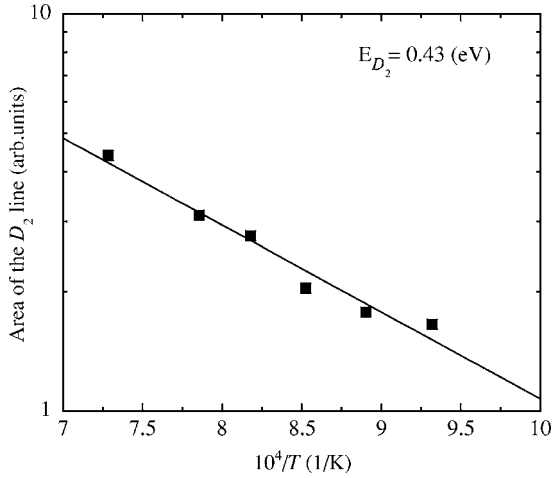

FIG. 7. Arrhenious plot of the area of D_2 line versus the inverse temperature in the temperature range from 800 to 1300 °C. Each area is obtained from the curve fitted result. From the slope of the least-squares fitted line, the activation energy of the D_2 formation was estimated to be 0.43±0.02 eV within 95% confidence interval.

and the optical band gap are markedly larger than that of the frozen-in structural disorder.

B. D_1 and D_2

In Fig. 5, it has been found that the D_2 intensity in F5 explicitly increases above 700 °C because of the progress of structural relaxation. It is considered that the D_1 intensity has the same tendency in essentials, because after cooling to room temperature the D_1 intensity as well as D_2 definitely increased as a consequence of frozen-in structure at higher temperature than the initial T_f. Unfortunately, since the overlapping SiF(ν_b) peak at 480 cm^{-1} could not be resolved from D_1 in the fitting procedure and its intensity may simply decrease with T, a clear observation like that of the D_2 intensity could not be made in Fig. 5.

The area of the D_2 line in F5 versus the inverse temperature shows the Arrhenious behavior in the temperature range from 800 to 1300 °C, as shown in Fig. 7. From the slope of the least-squares fitted line, the activation energy of the D_2 formation was estimated to be 0.43±0.02 eV within a 95% confidence interval. This value is very close to the previously reported values, 0.44,[23] 0.40,[12] 0.41 eV,[24] and all of which were estimated by using T_f evaluated at room temperature, not in terms of the measured T. In this study, we have first succeeded in determining the D_2 formation energy from the *in situ* measurement.

The discontinuous change of D_2 (D_1) intensity above T_g matches with the results of *in situ* light scattering[2] and *in situ* SAXS.[3] It implies that the dynamical configuration changes accompanied by the formation of D_1 and D_2 structures strongly influence the density fluctuations at high temperatures, but is less sensitive to the rate of change of the Si-O-Si average bond angle.

C. Quantitative estimate of θ change with T

The estimate of θ using vibrational spectroscopy has been subjected to study for years.[12,25–29] For the IR spectroscopy,

Lehmann *et al.*[25] theoretically predicted all the frequencies of fundamental vibrations including TO-LO splitting by using the parameters of the Born potential as well as the short-range force with both central and noncentral force constants.

The calculated IR frequencies are in good agreement with corresponding results in not only the IR but the Raman experiments. For example, the silicon bending (ω_B) and the Si-O asymmetric stretching (ω_S) motions correspond to the 800- and 1100-cm^{-1} peaks in the IR spectrum, respectively, while to ω_3 and ω_4 in the Raman spectrum as it is, respectively, whereas, the oxygen rocking (ω_R) motion, corresponding to the low-frequency peak at about 450 cm^{-1}, is dominantly IR active and is predicted only by using the noncentral force constant. If the noncentral force constant can be evaluated separately from ω_R, the accuracy of estimating θ from frequency ω_4 or ω_3 of the Raman spectra may be improved instead of by using the equations of ω_S or ω_B. However, it is very difficult experimentally to obtain ω_R, i.e., the noncentral force, and its temperature dependence. In addition, because of asymmetric peak shape and overlap with other peaks in the Raman spectrum, it is more difficult to deal with ω_1 and ω_3 than ω_4, in comparison to the theoretically predicted values. As previously pointed out in Refs. 10–12, CFNM is an approximate method because it completely ignores the noncentral force. Meanwhile, there has been no alternative model proposed for decades. Consequently at this moment, in order to compare the T to T_f dependence of θ, the use of ω_4 with CFNM is considered to be the most expedient in the Raman experiment. Thus, hereinafter, we evaluate the quantitative change of θ from ω_4 by following CFNM.

By differentiating Eq. (4) with respect to temperature, the following equation is derived:

$$\frac{\Delta\theta}{\Delta T} = \frac{2m_O\omega_4}{\alpha \sin\theta}\frac{\Delta\omega_4}{\Delta T} - \frac{1}{\alpha \sin\theta}\left(1 - \cos\theta + \frac{4m_O}{3m_{Si}}\right)\frac{\Delta\alpha}{\Delta T}. \quad (5)$$

It is assumed that α may be dependent on temperature because of the elongation of the Si-O bond length by thermal expansion. We utilize here an experimental law found by Badger,[30]

$$\alpha(L_0 - k_{ij})^3 = 1.86 \times 10^2, \quad (6)$$

where L_0 is the bond length and k_{ij} is a constant depending only on the rows in the periodic table in which the two elements comprising a molecule are located. In the case of Si-O bonding, L_0 is 1.62 Å, and k_{ij} is 0.90 according to Ref. 30. Then, differentiating with respect to temperature yields

$$\frac{\Delta\alpha}{\Delta T} = -\frac{5.58 \times 10^2 L_0}{(L_0 - k_{ij})^4}\left(\frac{\Delta L/L_0}{\Delta T}\right). \quad (7)$$

In Eq. (7), $(\Delta L/L_0)/\Delta T$ corresponds to the linear thermal-expansion coefficient. By substituting Eq. (7) into Eq. (5), the temperature dependence $\Delta\theta/\Delta T$ can be obtained.

For estimating $\Delta\theta/\Delta T$, in comparison with the T_f dependence of θ, $\Delta\theta/\Delta T_f$, we absolutely followed the procedures and parameters by Geissberger *et al.*[12] α=545 N/m and θ =130° were used, resulting in ω_4=1175 cm^{-1} in Eq. (4). Since the returned ω_4 is close to the measured ω_4(LO), the slope of ω_4(LO) shown in Table II, was used as $\Delta\omega_4/\Delta T$ in Eq. (5). The value $(\Delta L/L_0)/\Delta T$ was quoted from Ref. 31, 5×10^{-7}/°C for ND and 3×10^{-7}/°C for F5, respectively.

As a result, $\Delta\theta/\Delta T$ was estimated to be −0.022°/°C for ND and −0.023°/°C for F5, respectively. Correspondingly, on the assumption that α is constant, $\Delta\theta/\Delta T_f$ was estimated to be −0.0052°/°C for ND and −0.0046°/°C for F4, respectively, which were comparable with a previously predicted value in pure silica glass,−0.0057°/°C.[12] That is, even after additionally taking into account the temperature dependence of α accompanied by thermal expansion, it was evaluated that $\Delta\theta/\Delta T$ is a few times higher than $\Delta\theta/\Delta T_f$.

From XRD and NMR analysis, the average Si-O-Si bond angle in silica glass is approximately 144° and is thought to range from 120° to 180°, at room temperature.[32,33] Simply according to the obtained $\Delta\theta/\Delta T$, the deviation of θ at 1000 °C is predicted to be about −20° from the value at room temperature. Because the rate of θ change tends to become higher when estimated from ω_4 in CFNM as shown in details in Ref. 12, there still remains room for argument on the validity of absolute value. However, as far as was analyzed in the same way, it is definitely predicted that $\Delta\theta/\Delta T$ is a few times higher than $\Delta\theta/\Delta T_f$. The fact is quite significant for understanding the microscopic structural changes in silica glass occurring with the increase of temperature as follows.

First, it is reported that θ decreases by a few degrees at room temperature when T_f increases by about 500 °C.[5,12] In contrast, at elevated temperatures, it is possibly considered that $\Delta\theta$ largely goes beyond the bounds even below T_g, to maintain the structure with thermal expansion in the glassy state. When the temperature further rises over the T_g in the supercooled liquid state, θ still continues to decrease at nearly the same rate and structural relaxation occurs, resulting in the increase of the so-called D_1 and D_2 structures. Finally, when quenched to room temperature, θ almost inversely increases but can no longer return to the initial angle because of the history of structural relaxation, being a smaller angle than the initial. The angular difference is dependent on ΔT_f.

The above-described mechanism leads to a simple view that the much larger decrease of θ at high temperatures than ever expected may be most necessary for the dynamical atomic configuration changes, i.e., the formation of D_1 and D_2 structures. Furthermore, it helps us to realize the simple fact that θ decreases with the increase of T_f.

V. CONCLUSION

In this paper the structural changes of silica glass were quantitatively investigated as a function of temperature with *in situ* Raman spectroscopic measurement. From the frequency shift of fundamental vibrations, it was deduced that the decreases of both the Si-O-Si average bond angle θ and the Si-O bond-stretching force constant α simultaneously occur by thermal expansion. It was made clear that the rates of change of band frequencies with temperature are definitely

less sensitive to T_g contrary to a previous report, while the D_2 (and D_1) intensity explicitly increases above T_g. The activation energy of D_2 formation was determined by using actual temperature to be 0.43 ± 0.02 eV, by utilizing an F-doped silica glass having a low T_g. The value is close to the previously obtained ones by using T_f evaluated at room temperature in pure silica glass. It was estimated from CFNM and Badger's law that $\Delta\theta/\Delta T$ is a few times larger than $\Delta\theta/\Delta T_f$. To conclude, it was suggested that the much larger decrease of θ at high temperatures than ever expected may be most necessary for the dynamical atomic configuration changes, i.e., the formation of D_1 and D_2.

[1] R. Bruckner, J. Non-Cryst. Solids **5**, 123 (1970).
[2] K. Saito and A. J. Ikushima, Appl. Phys. Lett. **70**, 3504 (1997).
[3] C. Levelut, A. Faivre, R. Le Parc, B. Champagnon, J.-L. Hazemann, L. David, C. Rochas, and J.-P. Simon, J. Non-Cryst. Solids **307–310**, 426 (2002).
[4] K. Saito and A. J. Ikushima, Phys. Rev. B **62**, 8584 (2000).
[5] A. Agarwal, K. M. Davis, and M. Tomozawa, J. Non-Cryst. Solids **185**, 191 (1995).
[6] H. Kakiuchida, K. Saito, and A. J. Ikushima, Jpn. J. Appl. Phys., Part 1 **42**, 6516 (2003).
[7] T. Watanabe, K. Saito, and A. J. Ikushima, J. Appl. Phys. **94**, 4824 (2003).
[8] K. Saito and A. J. Ikushima, J. Appl. Phys. **91**, 4886 (2002).
[9] N. Shimodaira, K. Saito, N. Hiramitsu, S. Matsushita, and A. J. Ikushima, Phys. Rev. B **71**, 024209 (2005).
[10] P. N. Sen and M. Thorpe, Phys. Rev. B **15**, 4030 (1977).
[11] F. L. Galeener, J. Non-Cryst. Solids **49**, 53 (1982).
[12] A. E. Geissberger and F. L. Galeener, Phys. Rev. B **28**, 3266 (1983).
[13] M. D. Newton and G. V. Gibbs, Phys. Chem. Miner. **6**, 221 (1980).
[14] E. P. Markin and N. N. Sobolev, Opt. Spectrosc. **9**, 309 (1960).
[15] P. H. Gaskell, Trans. Faraday Soc. **62**, 1493 (1966).
[16] P. Richet and Y. Bottinga, Geochim. Cosmochim. Acta **48**, 453 (1984).
[17] P. F. McMillan, B. T. Poe, Ph. Gillet, and B. Reynard, Geochim. Cosmochim. Acta **58**, 3653 (1994).
[18] M. Kyoto, Y. Ohba, S. Ishikawa, and Y. Ishiguro, J. Mater. Sci. **28**, 2738 (1993).
[19] H. Kakiuchida, K. Saito, and A. J. Ikushima, J. Appl. Phys. **93**, 777 (2003).
[20] R. Shuker and R. W. Gammon, Phys. Rev. Lett. **25**, 222 (1970).
[21] F. L. Galeener and P. N. Sen, Phys. Rev. B **17**, 1928 (1978).
[22] V. N. Devisov, B. N. Mavrin, V. B. Podobedov, Kh. E. Sterin, and B. G. Varshal, J. Non-Cryst. Solids **64**, 195 (1984).
[23] J. C. Mikkelsen, Jr. and F. L. Galeener, J. Non-Cryst. Solids **37**, 71 (1980).
[24] N. Shimodaira, K. Saito, and A. J. Ikushima, J. Appl. Phys. **91**, 3522 (2002).
[25] A. Lehmann, L. Schumann, and K. Hubner, Phys. Status Solidi B **117**, 689 (1983).
[26] R. A. B. Devine and J. Arndt, Phys. Rev. B **35**, 9376 (1987).
[27] I. P. Lisovskii, V. G. Litovchenko, V. G. Lozinskii, and G. I. Steblovskii, Thin Solid Films **213**, 164 (1992).
[28] R. A. B. Devine, J. Non-Cryst. Solids **152**, 50 (1993).
[29] M. Tomozawa, J. W. Hong, and S. R. Ryu, J. Non-Cryst. Solids **351**, 1054 (2005).
[30] R. M. Badger, J. Chem. Phys. **2**, 128 (1934).
[31] A. Koike, Y. Iwahashi, N. Sugimoto, and S. Ito, *Proceedings of the XX International Congress on Glass*, O-07-051, 2004.
[32] R. L. Mozzi and B. E. Warren, Annu. Rev. Phys. Chem. **2**, 164 (1969).
[33] R. A. B. Devine, R. Dupree, I. Farnan, and J. J. Capponi, Phys. Rev. B **35**, 2560 (1987).